Structural Investigation of the Aqueous Eu 2+ Ion: Comparison with Sr 2+ Using the XAFS Technique

ARTICLE *in* THE JOURNAL OF PHYSICAL CHEMISTRY A · MARCH 2002

Impact Factor: 2.69 · DOI: 10.1021/jp0139639 · Source: OAI

4 AUTHORS, INCLUDING:

Lothar Helm
École Polytechnique Fédérale de Lausanne
240 PUBLICATIONS **7,719** CITATIONS
SEE PROFILE

Juris Purans
University of Latvia
220 PUBLICATIONS **1,844** CITATIONS
SEE PROFILE

André E Merbach
École Polytechnique Fédérale de Lausanne
463 PUBLICATIONS **14,032** CITATIONS
SEE PROFILE

Structural Investigation of the Aqueous Eu^{2+} Ion: Comparison with Sr^{2+} Using the XAFS Technique

Gilles Moreau,[†] Lothar Helm,[†] Juris Purans,[†,‡] and André E. Merbach*[,†]

Institute of Molecular and Biological Chemistry, Ecole Polytechnique Fédérale de Lausanne, EPFL-BCH, CH-1015 Lausanne, Switzerland, and Institute of Solid State Physics, Kengaraga str. 8, LV-1063 Riga, Latvia

Received: October 25, 2001

Structural parameters of the Sr^{2+} and, for the first time, of the Eu^{2+} ions in aqueous solution were determined by the XAFS method. For the Sr^{2+}, the use of an improved theoretical approach led to a first shell coordination number of 8.0 (3), a Sr−O distance of 2.600 (3) Å and a Debye−Waller factor of $\sigma^2 = 0.0126$ (5) Å^2. These results were confirmed by an analysis performed with experimental phase and amplitude, extracted from the solid reference compound $[Sr(H_2O)_8](OH)_2$. The same theoretical approach was used for the analysis of the Eu^{2+} XAFS spectra in aqueous solution. This gives a first coordination shell of Eu^{2+} formed by 7.2 (3) water molecules, an Eu−O distance of 2.584 (5) Å, and a high Debye−Waller factor of $\sigma^2 = 0.0138$ (5) Å^2. Whereas Eu^{3+} occurs as an equilibrium between the $[Eu(H_2O)_8]^{3+}$ and the $[Eu(H_2O)_9]^{3+}$ ions, Eu^{2+} occurs in aqueous solution as an equilibrium between a predominant $[Eu(H_2O)_7]^{2+}$ ion and a minor $[Eu(H_2O)_8]^{2+}$ species.

Introduction

Eu^{2+} is isoelectronic to Gd^{3+} and shows similar magnetic properties. The high magnetic moment ($S = 7/2$) of both ions, associated to relatively slow electron spin relaxation rates, makes them an ideal choice for nuclear magnetic relaxation enhancement,[1] a highly regarded property in contrast agents for medical magnetic resonance imaging.[2] Unfortunately, Eu^{2+} is unstable in aqueous solution[3] as it reacts quickly with oxygen and is slowly oxidized by water.[4] We have recently demonstrated that carefully prepared samples are sufficiently stable to be studied over several hours.[5] Little is known so far about the Eu^{2+} ions in aqueous solution.[6] By ^{17}O NMR, it has recently been found that Eu^{2+} shows the fastest water exchange process measured so far by this technique.[5] Because structural parameters of the first coordination shell, like the coordination number and the metal−oxygen distance, were unknown, assumptions had to be made on the basis of comparison with the available Sr^{2+} data.

Few direct methods are currently available to determine structural parameters such as the metal−water distance and the coordination number in aqueous solution. X-ray scattering needs highly concentrated solutions. Structural investigations using the neutron diffraction difference technique are based on the availability of pairs of isotopes with sufficiently different coherent neutron scattering lengths (for lanthanides: Nd, Sm, Dy, Yb).[7] As the stable ^{151}Eu and ^{153}Eu isotopes have too similar coherent scattering lengths, the neutron diffraction difference technique cannot be performed. The large angle X-ray scattering (LAXS) method gives weighted contributions of all interatomic distances in the sample. In aqueous solution, there is severe overlap between the metal−oxygen distances, and the water−water distances from the bulk, and a difference procedure must be applied.[8] The X-ray absorption fine structure (XAFS) method has become an important experimental method for the examination of the local atomic environment in both solid and liquid states.[9] Trivalent lanthanide ions in aqueous solution have been studied by XAFS during the past decade,[10,11] but only very recently has an X-ray absorption near-edge structure (XANES) been reported on the Eu^{2+} ion in solution.[12] It showed that white line positions and amplitudes differ substantially between di- and trivalent europium ions: the white line of Eu^{3+} appears in the energy region of Eu^{2+} XAFS. Therefore, even small amounts of Eu^{3+} present in solution make the analysis of Eu^{2+} XAFS spectra difficult, which may explain why no XAFS structural data of Eu^{2+} in aqueous solution have been published so far.

As Sr^{2+} is similar in size (ionic radii are, respectively, 1.25 and 1.26 Å for the octacoordinated Eu(II) and Sr(II) ions)[13] and shows a similar chemistry,[14] this alkaline earth metal is often used as an easy-to-handle model compound for the unstable europium(II) ion. In recent years, several studies on Sr^{2+} in aqueous solution using XAFS,[15−21] neutron[22] and X-ray[23] diffraction, and molecular dynamics simulation[24,17,21] have been performed. Unfortunately they showed widespread results concerning Sr−O distances as well as coordination numbers (from 7 to 10).

In the present work, the experimental L_3-edge XAFS spectra of Eu^{2+} in aqueous solutions as well as the Sr^{2+} K-edge have been measured, analyzed, and compared using the cumulant approach combined with efficient analysis techniques.[25,26] Both theoretical (calculated ab initio[27]) and experimental (extracted from aqua ion crystalline reference[28]) phases and amplitudes have been used.

Experimental Section

Chemicals. $[Eu(H_2O)_9](O_3SCF_3)_3$ was prepared as described in the literature.[29] $[Sr(H_2O)_8](OH)_2$ crystalline compound (98%) was purchased from Acros. Both compounds were checked by single-crystal X-ray diffraction.[29,16] 98% CF_3SO_3H (triflic acid) was purchased from Aldrich Chemicals. All commercial compounds were used as received.

Preparation of the Samples. An Eu^{3+} aqueous solution (0.15 M) was prepared by dissolution of the trifluoromethansulfonate

* Author to whom correspondence should be addressed. Phone: +41-21-693 98 71. Fax: +41-21-693 98 75. E-mail: andre.merbach@epfl.ch.
† Ecole Polytechnique Fédérale de Lausanne.
‡ Institute of Solid State Physics.

10.1021/jp0139639 CCC: $22.00
Published on Web 03/03/2002

(triflate) salt into diluted triflic acid (5×10^{-2} M). The strontium triflate solution (0.14 M) was obtained by dissolution of the hydroxide salt in water followed by addition of an excess of 98% triflic acid (final acid concentration: 5×10^{-2} M).

The Eu^{2+} solutions were prepared electrochemically from an europium(III) triflate stock solution (0.15 M) in 0.1 M triflic acid using controlled potential coulometry in a homemade electrolysis cell[14] at a potential of −0.9 V vs Ag/AgCl. After complete reduction, the samples were taken out with a syringe and filled into a round-bottom flask, sealed with a septum to avoid oxygen contamination. Additionally, the solutions were treated by amalgamated zinc just before the XAFS measurements to avoid traces of Eu^{3+}. The 5% amalgamated zinc pellets[30] were prepared from analytical grade zinc purchased from Merck. Eu^{2+} concentrations were checked using the procedure described elsewhere.[14] The L_3-edge XANES measurements (see below) have confirmed that sealed oxygen-free samples of Eu^{2+} (0.15 M) aqueous solutions are stable in the multipurpose cell we used for at least 5 h.

The reference crystalline sample $[Sr(H_2O)_8](OH)_2$ was finely ground and mechanically mixed with cellulose powder under nitrogen atmosphere to give pressed pellets with thickness chosen to obtain an absorption jump value of about 1.

To avoid oxidation of Eu^{2+} samples and carbonation of $[Sr(H_2O)_8](OH)_2$, manipulations were performed under nitrogen or argon atmosphere.

XAFS Measurements. XAFS measurements of europium and strontium solutions were performed on the beam line BM29 of the 3rd generation synchrotron radiation facility ESRF (Grenoble, France). Electron-beam energy and average current were 6.0 GeV and 200 mA, respectively. The XAFS spectra of the Eu L_3-edge (6976 eV; scan 6900−7650 eV) and Sr K-edge (16105 eV; 16 000−17 000 eV) were measured in transmission mode. The synchrotron radiation was monochromatized using the Si(111) double-crystal monochromator and 50% of harmonic rejection was achieved by slightly detuning the two crystals from parallel alignment. The experimental spectra were measured using two ionization chambers (He + N_2 mixture for Eu, and He + Ar mixture for Sr measurements) with a variable step in the wave-vector range of 0.025 $Å^{-1}$, a count rate of 1 s per point, and an energy resolution of 0.7 eV. The white line (WL) edge positions were reproducible with a precision better than 0.1 eV. A multipurpose X-ray absorption cell[31] was used for the in-situ XAFS measurements of sealed oxygen-free solutions. The measurements were done at an optical length of 1 mm for Eu and 4 mm for Sr, resulting in values of the absorption jump of about 0.5 (WL amplitude about 2) for Eu and about 1 for Sr. To estimate the saturation effect on the WL amplitude, additional measurements for europium solutions were done at different optical lengths (1, 1.5, and 2 mm). At least two complete and identical XAFS scans were collected for each solution. The kinetics of the Eu^{2+}oxidation was followed by 10 successive scans in the XANES region.

Additional strontium solution measurements and all the solid-state strontium XAFS spectra were recorded at LURE (Orsay, France) on the DCI D42 (XAFS 13) beam line (1.85 GeV and 320 to 250 mA) on the Sr K-edge (16105 eV; scan 16000−17200 eV). The synchrotron radiation was monochromatized using a Si(331) channel-cut monochromator. The experimental spectra were measured by two ionization chambers filled with Ar with a count rate of 1 to 3 s per point. The solution sample was measured in the same multipurpose X-ray absorption cell with an optical path length of 4 mm resulting in an absorption jump of about 1. All samples were measured at room temperature.

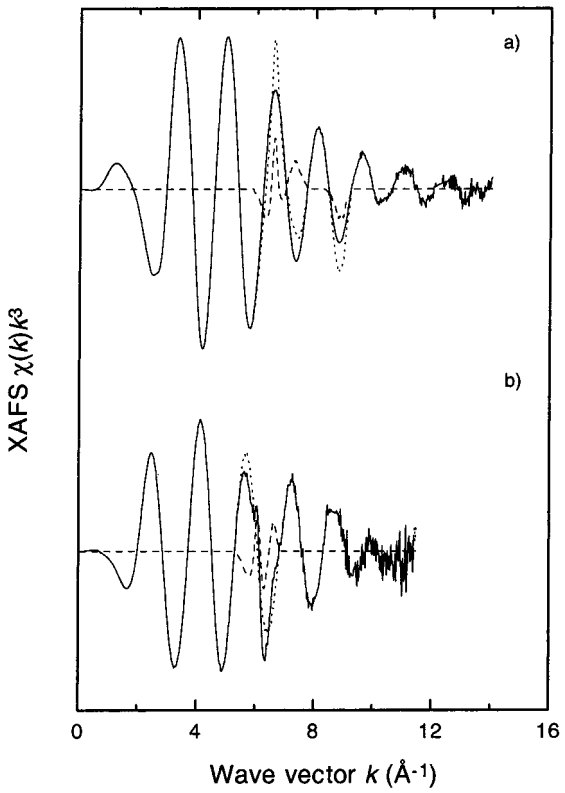

Figure 1. Comparison between the experimental XAFS spectra before (···) and after correction (—) for the multielectron transition contributions (- - -) both for (a) 0.14 M Sr^{2+} and (b) 0.15 M Eu^{2+} ions in aqueous solution.

Data Analysis. The experimental XAFS data were treated using the EDA software package.[32] The X-ray absorption coefficient $\mu(E) = \ln(I_0/I)$ was obtained from the intensities of the synchrotron radiation, measured before (I_0) and after (I) the sample. Particular attention was devoted to the XAFS zero-line removal (background and multielectron contributions) through a multistep polynomial/cubic-spline procedure.[33] The obtained XAFS spectra, $\chi(E)$, were converted to the k-space of the photoelectron wavevector, defined as $k = \sqrt{(2m/\hbar^2)}(E - E_0)$, where $(E - E_0)$ is the photoelectron kinetic energy measured. In the case of the L_3-edge of rare earth elements, E_0 is located at energies higher than the white line.[34] For Eu^{3+} and Eu^{2+} the energies E_0 were located at ca. 2 eV above the white line maxima. For Sr, the energy E_0 was located above the first inflection point and about 3 eV below the maximum. The experimental XAFS spectra $\chi(k)$ of both Eu and Sr were multiplied by a factor k^3 to compensate for the decrease of amplitude with increasing wave-vector value.

The experimental XAFS spectra were Fourier transformed (FT) with a Kaiser-Bessel window in the 0−14 $Å^{-1}$ range for both Eu and Sr. The experimental spectra were compared with the corresponding first shell XAFS spectrum filtered by back Fourier transform in the 1.1−2.7 Å range for both Eu L_3-edge and Sr K-edge. The differences, or residual curves, show the presence of well-defined peaks (Figure 1) corresponding to multielectron transitions.[11,18] These peaks were removed from the experimental XAFS spectra on appropriate ranges, given in Table 1.

The resulting spectra were then Fourier transformed using a photoelectron phase shift correction, and the first shell XAFS contributions were singled out by back FT procedure in the 1.9−

TABLE 1: Multielectron Transition Positions, and Corresponding Corrected *k*-Ranges in the Experimental XAFS Spectra[a]

MET	position	corrected range
Sr K-edge *1s3d*	6.4	5.9−7.3
Sr K-edge *1s3p*	8.9	8.3−9.2
Eu L_3-edge *2p4d*	6.1	5.3−6.8

[a] Every value is given in $Å^{-1}$.

3.2 Å range for both Eu^{2+} and Sr^{2+}. Use of the phase shift correction (see below) allowed us to reduce the nonstructural peaks distorting the baseline, and led to a significant sharpening of the first shell peak (Figure 4), allowing a more precise Fourier filtering. The successive subtraction of multielectron transition contributions and the use of the corrected Fourier filtering procedure led to a real increase in the fitting reproducibility when changing the Δk fitting range.

The first-shell XAFS spectra were fitted using the single-scattering curved-wave formalism with cumulant expansion:[25]

$$\chi(k) = \frac{N}{kC_1^2} f(\pi,k) \exp\left(-\frac{2C_1}{\lambda(k)}\right) \exp\left(-2C_2k^2 + \frac{2}{3}C_4k^4\right) \sin\left(2kC_1 - \frac{4}{3}C_3k^3 + \phi(\pi, k)\right) \quad (1)$$

where N is the coordination number; $C_2 = \sigma^2$ is the Debye−Waller (DW) factor (in harmonic approximation). The higher-order cumulants C_3 and C_4 characterize the deviation of the distribution of distances from a Gaussian shape. The first cumulant C_1 is closely related to the interatomic distance R. To obtain the real mean distance R, the following expression[35] has to be applied:

$$R \cong C_1 + (2\sigma^2/C_1)\,(1 + C_1/\lambda) \quad (2)$$

This correction is particularly important for systems with a large DW factor, as for the Eu^{2+} and Sr^{2+} aqua ions. From calculated $\lambda(k)$ functions, the $1+C_1/\lambda$ term has been approximated to 1.2, leading to an uncertainty of 0.0005 Å on distances.

$\lambda(k) = k/\Gamma$ is an adjustable function that models the low k damping factors. The FEFF6 code[27] already includes in the calculated scattering amplitude functions $f(\pi,k)$ damping factors to take into account the photoelectron mean-free path and the core-hole level lifetime using the Hedin-Lundqvist potential. However, we allowed the Γ parameter to vary during the fitting procedure, for fine adjustment between these theoretical contributions and the experiment. This parameter also allows us to compensate for the FT boundary effects, or the resolution difference between spectra recorded at LURE or ESRF.

In this paper, the strontium XAFS data were analyzed using two different approaches: the phases $\phi(\pi,k)$ and amplitudes $f(\pi,k)$ were either calculated or obtained experimentally from a crystalline aqua ion reference.

Theoretical backscattering amplitudes and phases were calculated by the FEFF6 code[27] using different clusters that mimic the possible environment of the Eu^{2+} and Sr^{2+} ions in aqueous solutions, respectively. The choice of the clusters used will be discussed later in the article but were based in all cases on the $[Sr(H_2O)_8](OH)_2$ crystalline coordinates.[16]

As the threshold energy of the photoelectron E_0 is defined in the FEFF6 code[27] relative to the Fermi level and depends on the muffin-tin radii, the spectra have to be corrected to avoid E_0 difference errors in the fitting process. Consequently, the phase differences between theoretical and experimental spectra were set to zero at low k, according to Bunker and Stern's criterion,[36] and E_0 was allowed to vary for fine adjustment during the fitting procedure.

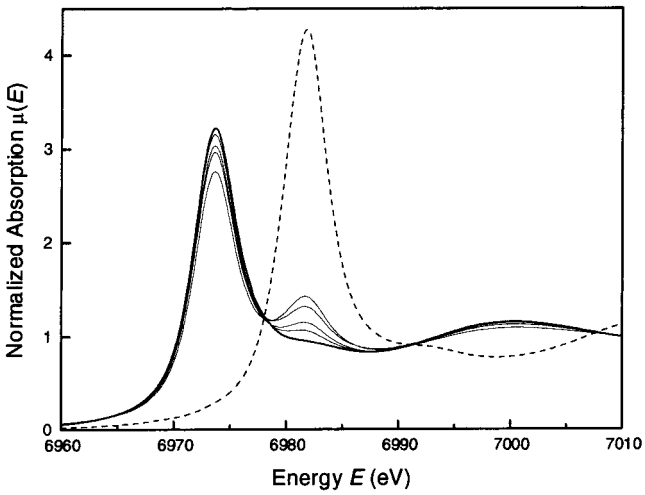

Figure 2. XANES spectrum of a 0.15 M Eu^{2+} solution just after treatment by amalgamated zinc (—), its evolution in an open cell showing oxidation by air (−), and XANES spectrum of a pure 0.15 M Eu^{3+} solution (- - -).

Experimental $f(\pi,k)$ and $\phi(\pi,k)$ were extracted from the experimental XAFS data obtained on the crystalline $[Sr(H_2O)_8](OH)_2$. These functions were obtained assuming Gaussian distribution with $N = 8$ and $R = 2.619$ Å, from the crystallographic data,[16] and $\sigma^2 = 0.0117$ $Å^2$ from the fit with theoretical phase and amplitude.

Note that use of experimental phases and amplitudes allows, to a certain extent, the compensation of systematic errors as they include the contribution of the mean free path, of the multielectron amplitude reduction factor S_0^2, of glitches and resolution, reducing the number of adjustable parameters, and consequently increasing the reliability of the fitted results. To ensure the phases and amplitudes transferability, and to allow estimation of systematic errors, all the data were analyzed in a similar way, using the same theoretical phases and amplitudes, filtering procedures and parameters.

Results and Discussion

Eu^{3+} Contamination. It was early recognized that the two valence states of $Eu^{2+}(4f^7)$ and $Eu^{3+}(4f^6)$ can be easily distinguished by XANES spectroscopy due to the different threshold energies (about 8 eV) of their white line (WL) resonance which correspond to the transition to the unoccupied 5d-states.[37,38] The basic reason for this difference is the lower binding energy of the respective core electrons caused by the shielding of the nuclear potential through the additional 4f-electron.[37] The experimental XANES spectra (Figure 2) on the Eu L_3-edge of Eu^{2+} and Eu^{3+} aqueous solutions are in good agreement with recently published results.[12] The Eu^{2+} XANES spectrum consists of a dominant WL (normalized amplitude 3.2 at 6974 eV) and a very weak peak around 6982 eV. This peak can be attributed either to the traces of Eu^{3+} ion (WL) or to multiple-scattering effects or to a combination of both. Note that the Eu^{3+} aqua ion XANES spectrum consists of a WL with normalized amplitude 4.3 at 6982 eV and also a weak peak at ca. 6994 eV, commonly attributed to multiple-scattering effects.[39] By analogy, it is reasonable to consider that the very small peak present in the Eu^{2+} solution treated with amalgamated zinc can be attributed solely to multiple scattering effects and no more to Eu^{3+} contamination. No oxidation occurs in the XANES spec-

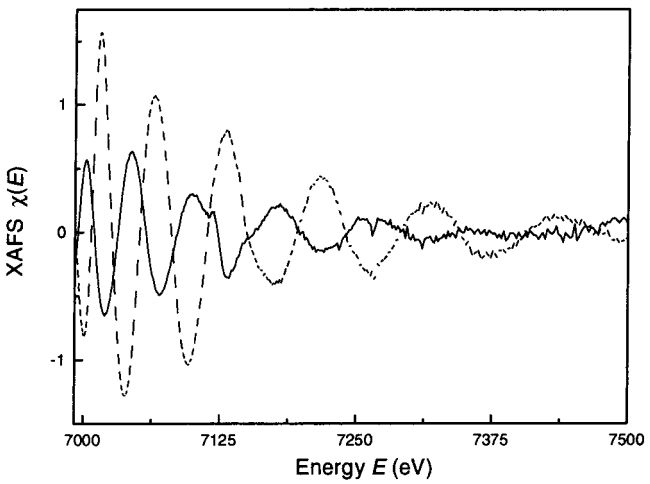

Figure 3. Experimental XAFS spectrum vs energy of 0.15 M Eu^{2+} (−) and 0.15 M Eu^{3+} (− − −) aqueous solutions, showing destructive interference between the experimental Eu^{2+} and Eu^{3+} spectra.

trum of the freshly reduced Eu^{2+} solution after 1 h of measurement. If we assume the freshly reduced solution to be free of Eu^{3+} ions, we can estimate the Eu^{3+} contamination after 5 h to ca. 2%. A further reduction by addition of amalgamated zinc leads to the original spectrum, confirming the multiple scattering hypothesis.

In situ XANES measurements after exposure of the solution to oxygen show a decrease with time of the Eu^{2+} WL (6974 eV) and an increasing amplitude of the peak at 6982 eV (Figure 2). This is a clear indication of Eu^{2+} oxidation to Eu^{3+}. From the different sets of data collected for contaminated Eu^{2+} solutions, we can evaluate the maximum quantity of Eu^{3+} present in the freshly reduced Eu^{2+} solution to less than 1%.

The experimental XAFS spectra $\chi(E)$ of the Eu^{2+} and Eu^{3+} aqueous solutions show destructive interference when plotted versus an energy scale (Figure 3) due to their different E_0 energies ($\Delta E_0 \sim 8$ eV). Additionally, we observe that the Eu^{3+} XAFS spectrum is about twice as high as the Eu^{2+} one, for the same europium concentration. Consequently, even traces (down to 5%) of Eu^{3+} in solution make the analysis of Eu^{2+} XAFS spectra very difficult and can lead to a misinterpretation of the data and wrong coordination numbers and distances. This may explain why no XAFS data of Eu^{2+} in aqueous solution have been published so far whereas XANES results are present in the literature.[12]

Strategy for the Choice of the XAFS Reference. A widespread range of coordination numbers is reported for the Sr^{2+} ion in aqueous solution, from 7.3 to 10.3, with a majority of values around 8.[15,18] Attempts to determine the coordination number of metal aqua ions *without* using appropriate calibration compounds may give large errors.[16] A good reference should provide the metal center with a local environment which mimics its environment in aqueous solutions,[46] e.g., an 8-coordinated aqua ion with a narrow distribution of distance. The octahydrated strontium hydroxide $[Sr(H_2O)_8](OH)_2$ is the best candidate as it crystallizes in the solid state with a Sr^{2+} ion surrounded by eight water molecules in a distorted square antiprism with a mean distance of 2.619 Å (corresponding to two distances of 2.613 and 2.625 Å) and 24 oxygen atoms from 4.630 to 4.875 Å, from both hydroxide ions and second sphere water molecules.[16]

The corresponding Eu^{2+} compound has not been isolated yet. Only a monohydrated europium(II) hydroxide has been obtained, but it reacts with water to yield $Eu(OH)_3$. To find an alternative europium(II) experimental reference, XAFS spectra were recorded for the hexacoordinated SrO,[40] the octacoordinated $SrSO_4$[41] and the enneacoordinated $[Sr(H_2O)_6]Cl_2$[42] and $SrCO_3$,[43] as they are supposedly isostructural to their europium(II) homologues.[44,45] All but the oxide proved to have too large a distribution of distances to allow the extraction of transferable phase and amplitude functions.

However, cubic SrO containing only one distance in the first shell is not a very good reference for the aqueous solution, as it is 6-fold coordinated and possesses a rather short Sr−O distance. As Palmer et al.[17] found that the coordination number of 7.7 was increased by 3−4 when using experimental phases and amplitudes from SrO instead of the SrO-like cluster (with Gaussian formalism), we can reasonably think that the use of EuO experimental $f(\pi,k)$ and $\phi(\pi,k)$ will neither confirm nor invalidate the coordination obtained with Eu L_3-edge theoretical phases and amplitudes.

Until now, no europium(II) crystal pure and stable enough to be used as an XAFS reference compound has been obtained. However, for the strontium solution, we have found an excellent agreement between the structural parameters obtained using phases and amplitudes extracted from solid $[Sr(H_2O)_8](OH)_2$, on one hand, and from a purely theoretical approach, on the other. This agreement validates the theoretical approach for the Sr^{2+} aqua ion, and allows us to use a similar approach for the Eu^{2+} aqua ion, based on the $[Eu(H_2O)_8](OH)_2$ cluster.

Multielectron Transition Effect. A number of authors[15,16,18] have already mentioned the presence of anomalous features in the Sr^{2+} aqua ion XAFS spectrum. Persson[16] encountered difficulties in determining a coordination number because of a "curious feature" at ca. 6.4 $Å^{-1}$, with a shape that cannot be modeled by normal curve-fitting.[16] Having no plausible explanation, but suspecting an electronic transition origin, he resolved to fix the coordination number to 8 when fitting the experimental XAFS curves. D'Angelo et al.[18] proved that these anomalies originated from the simultaneous excitation of *1s4s*, *1s3d*, and *1s3p* electrons and led to distortions in the XAFS spectrum at about 3.4, 6.4, and 8.9 $Å^{-1}$, respectively. In most cases, the multielectron transitions (MET) do not disturb the XAFS analysis, as their intensities are low, compared to the oscillations amplitude. In our case, these anomalies result after Fourier transform in humps distorting the base of the major peak standing for the first sphere Sr−O peak, especially at low distances. These humps prevent good first shell filtering of the experimental XAFS spectra by back Fourier transform, and induce an even greater distortion in the resulting curve.

The presence of sharp contributions modifying the fine structure beyond the absorption edge and consequently distorting the XAFS spectrum have also been reported in the case of the tripositive rare-earth L_3 edges and attributed to *2p4d* double-electron transitions.[11] Figure 1b shows that similar MET features are found for the Eu^{2+} solution at ca. 6.1 $Å^{-1}$.

These distortions increase the error in the determination of the structural parameters, and also decrease the fitting reproducibility when changing the Δk fitting range. The multielectron excitation background being not properly described by the standard multistep polynomial/cubic-spline functions used in zero-line removal procedures,[18] we decided to remove the anomalous distortions following a procedure analogous to the one used by Solera et al.[11] This procedure, combined with the phase shift corrected Fourier filtration, allowed us to lower our fitting errors by 1 order of magnitude. The fittings performed without MET removal show a 10% increase of the coordination number. The quality of the removal procedure can be checked

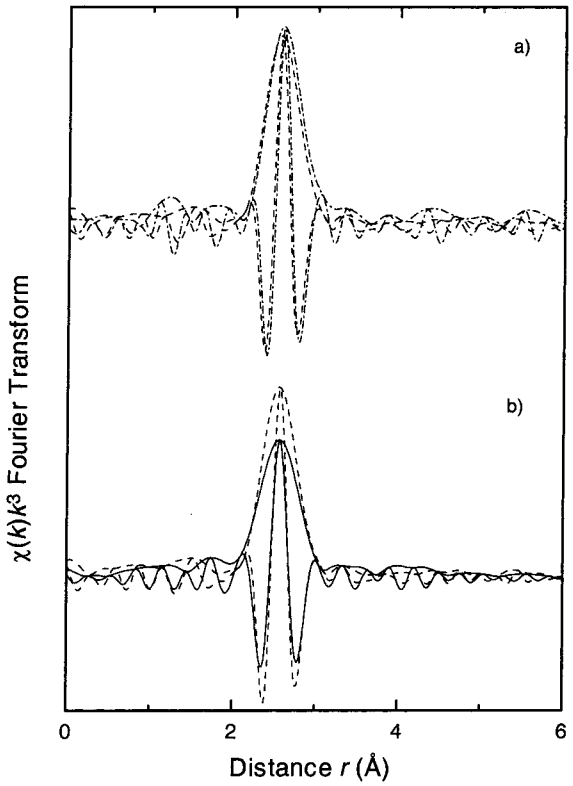

Figure 4. Comparison between Fourier transforms (modulus and imaginary parts) of the experimental XAFS $\chi(k)k^3$ spectra of: (a) 0.14 M Sr^{2+} solution (− − −) and solid $[Sr(H_2O)_8](OH)_2$ (−•−•−) (LURE), (b) 0.14 M Sr^{2+} (− − −) and 0.15 M Eu^{2+} (−) solutions (ESRF). These Fourier transforms have been corrected for the photoelectron phase shift using the theoretical phase and amplitude, and the Eu^{2+} solution imaginary part has been inverted for clarity.

directly by a simple Fourier transform, with the disappearance of the nonstructural peaks (Figure 4) previously observed by Pfund (Figure 4 of ref 15), Persson (Figure 8a of ref 16), D'Angelo (Figure 2 of ref 18) and Parkman (Figure 6 of ref 20).

Influence of the Hydrogen Atoms in Cluster Calculations. Due to the lack of an appropriate solid reference compound for the study of Eu^{2+} solutions, it is extremely important to determine the theoretical phase and amplitude with the highest absolute accuracy. The methodology will be tested on a strontium solution for which a good solid reference compound is available. To obtain good theoretical phases and amplitudes, the choice of an appropriate cluster is crucial. Palmer et al.[17] concluded, after extensive calculations performed on Sr^{2+} clusters with ca. 20 water molecules taken from Molecular Dynamics simulations, that the presence of hydrogen atoms on the water molecules distorts the FEFF6 theoretical calculations and leads to an underestimation of the coordination number by 2 or 3. As the $[Sr(H_2O)_8](OH)_2$ mimics best both the first and second hydration shell of the strontium aqua ion in solution, we tested several approaches on the basis of its crystal structure coordinates[16] with (a) all the oxygen and hydrogen atoms, i.e., $Sr(OH_2)_8(H_2O)_{16}(OH)_8$ (**1**); (b) all the oxygen and only the second sphere hydrogen atoms, i.e., $SrO_8(H_2O)_{16}(OH)_8$ (**2**); (c) only the SrO_8O_{24} cluster (**3**); (d) only the SrO_8 cluster (**4**). Figure 5 compares the FEFF6 calculations for the XAFS first shell contribution of these clusters to the experimental $[Sr(H_2O)_8](OH)_2$ spectrum. The calculated curve closest to the experimental reference is the cluster **2**, with all the oxygen atoms and only the second sphere hydrogen atoms.

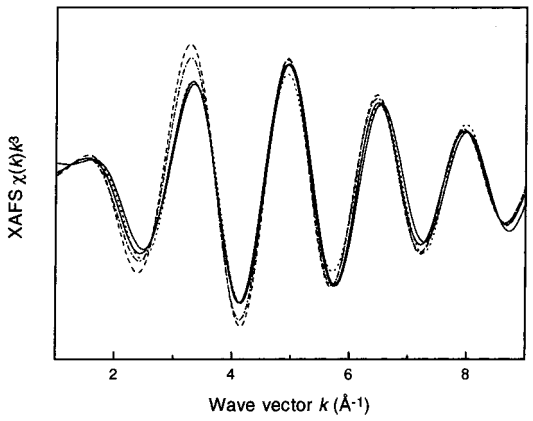

Figure 5. Experimental XAFS spectrum of the $[Sr(H_2O)_8](OH)_2$ solid compound (—) compared with the theoretically calculated spectra based on the following clusters: $Sr(OH_2)_8(H_2O)_{16}(OH)_8$ (**1**: − − −), $SrO_8(H_2O)_{16}(OH)_8$ (**2**: −), SrO_8O_{24} (**3**: ···), and SrO_8 (**4**: •−•−). These curves have been corrected for the experimental threshold energy E_0 and DW factor.

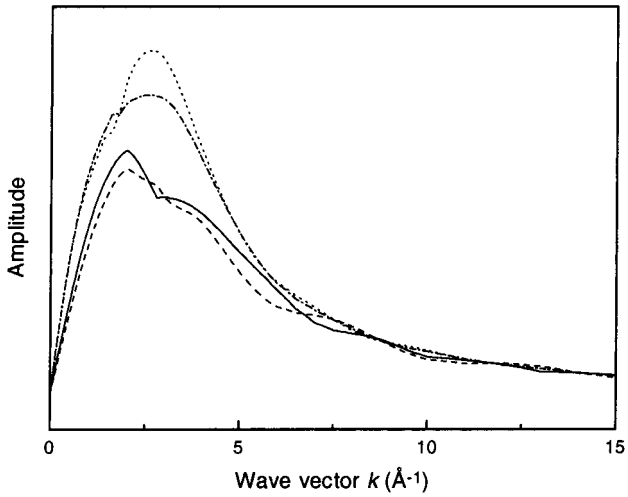

Figure 6. Theoretical backscattering amplitudes calculated by the FEFF6 program including mean free path damping factor $\exp(-2R/\lambda)$ for the following clusters: $Sr(OH_2)_8(H_2O)_{16}(OH)_8$ (**1**: − − −), $SrO_8(H_2O)_{16}(OH)_8$ (**2**: −), SrO_8O_{24} (**3**: ···) and SrO_8 (**4**: •−•−).

TABLE 2: Muffin-Tin Radii (R_{MT}) for the First Coordination Shell Atoms[a]

calculation	cluster	R_{MT} (Sr)	R_{MT} (O)
1st and 2nd shell H	1	1.610	0.678
2nd shell H only	2	1.491	1.143
SrO_8O_{24}	3	1.467	1.209
SrO_8	4	1.448	1.166

[a] All the muffin-tin radii are given in Å.

Figure 6 shows that the theoretical amplitude functions, calculated by the FEFF6 program are significantly influenced by the presence of hydrogen atoms (due to mean free path damping factors). This is not surprising as inelastic scattering processes are dominated by weakly bound electrons.[46] Moreover the presence of hydrogen atoms leads to an anomalous decrease of oxygen muffin-tin (MT) radius in the FEFF6 program from about 1.2 to ca. 0.7 Å (Table 2), whereas they are not supposed to take part in the Sr−O scattering phenomenon. As the MT approximation starts from overlapped spherically averaged relativistic atomic charge densities, the presence of close hydrogen atoms lowers the first sphere oxygen MT radius, and consequently increases the strontium MT radius (by at least 0.1

TABLE 3: First Coordination Shell Structural Data Obtained from XAFS Analysis of Sr^{2+} and Eu^{2+} Aqua Ions at Room Temperature[a]

sample	fit	N	C_1 (Å)	R (Å)	C_2 (Å^2)	C_3 (Å^3) $\times 10^{-4}$	ΔE_0	Γ	Δk	$\epsilon \times 10^{-3}$
Fit with Experimental Phase and Amplitude from the Solid $[Sr(OH_2)_8](OH)_2$ Reference Compound										
Sr^{2+} solution LURE	I	7.92 (3)		2.600 (1)	0.0126 (1)	1.8 (2)			1−11	1.2
Sr^{2+} solution ESRF	II	8.13 (3)		2.601 (3)	0.0127 (1)	2.6 (5)			2−11	3.5
Fit with Theoretical Phase and Amplitude										
$[Sr(OH_2)_8](OH)_2$	III	7.95 (5)	2.604 (1)	2.615 (2)	0.0117 (1)	1.1 (2)	−0.75	−0.052 (2)	2−12	1.5
Sr^{2+} solution LURE	IV	7.8 (3)	2.588 (2)	2.599 (3)	0.0124 (2)	2.6 (3)	−0.8	−0.04 (2)	3−10	3.5
Sr^{2+} solution ESRF	V	8.0 (1)	2.587 (1)	2.599 (2)	0.0125 (2)	2.8 (2)	−0.7	−0.08 (1)	2−13	0.8
Eu^{2+} solution ESRF	VI	7.0 (2)	2.570 (3)	2.583 (3)	0.0135 (3)	1.5 (3)	0		2−12	1.6

[a] N is the number of atoms located in the first shell at a distance R from the metal, C_1 is the first cumulant, $C_2 = \sigma^2$ is the DW factor, C_3 is the third cumulant characterizing the asymmetry of the RDF, ΔE_0 is the difference between experimental and theoretical E_0, Γ is a parameter related to the core-hole lifetime, Δk is the fitting interval, and ϵ is the fitting error.[33] Statistical errors are presented within brackets.

Å). By removing the hydrogen atoms of the first sphere water molecules, the two MT radii remain unchanged and a realistic amplitude function is obtained. The eight hydroxide hydrogen atoms of the 2nd shell are pointing toward the first sphere oxygen atoms,[16] and recreate a realistic inelastic scattering background. The presence of this hydrogen pseudo-layer located about 1 Å farther than the actual first sphere water hydrogen atoms seems to compensate to a certain extent for the flaws of the model, and reproduces well the experimental spectrum as was shown in Figure 5.

As a consequence, cluster **2** was chosen as a reference to analyze the strontium K-edge spectra. For the Eu L_3-edge, a similar cluster, with all the oxygen atoms and only the second sphere hydrogen atoms around the Eu^{2+} ion was used, and a scaling factor of 0.99 was applied to take into account the radius contraction from Sr^{2+} to Eu^{2+}.[13]

Results for the Sr^{2+} Aqua Ion. The FT of the Sr experimental XAFS spectrum in both solution and solid state consists of only one contribution near 2.6 Å, corresponding to the first coordination shell (Figure 4a). In the liquid phase, the absence of any significant contribution from the second hydration shell and from the multiple scattering in the XAFS FT is due to a highly disordered first shell and a diffuse second sphere, as already shown by Persson's[16] LAXS measurements. In the solid $[Sr(H_2O)_8](OH)_2$, the presence of strong thermal and structural disorder in the second coordination sphere (3 different Sr−O distances from 4.6 to 4.8 Å) explains the absence of such contributions, therefore, taking into account only the first coordination shell is sufficient in first approximation to interpret the experimental XAFS spectra in both states.

Table 3 summarizes the results from the analyses using both experimental and theoretical phases and amplitudes, and shows the good agreement of the two approaches in the case of the Sr^{2+} aqua ion. The experimental XAFS spectra $\chi(k)k^3$ after first shell filtering and the corresponding spectra, calculated from the parameters presented in Table 3, are compared in Figure 7. The very low residual intensities (dotted lines) demonstrate the excellent quality of these fits. The statistical errors presented in Table 3 have been evaluated accounting for correlations among parameters, by extensive fittings of the experimental first sphere XAFS spectra, changing the fitting intervals. Outside the fitting intervals indicated in Table 3, the fitting errors were at least doubled.

One may wonder why we did not refine the structural parameters directly from the unfiltered data and why we went through a complex procedure of windowing, removal of multiple excitation contributions, and back Fourier transforming. In fact, we did try to analyze directly the unfiltered data, but the fitted parameters were dependent on the Δk fitting range and on the fitting procedure. To obtain coherent structural parameters from

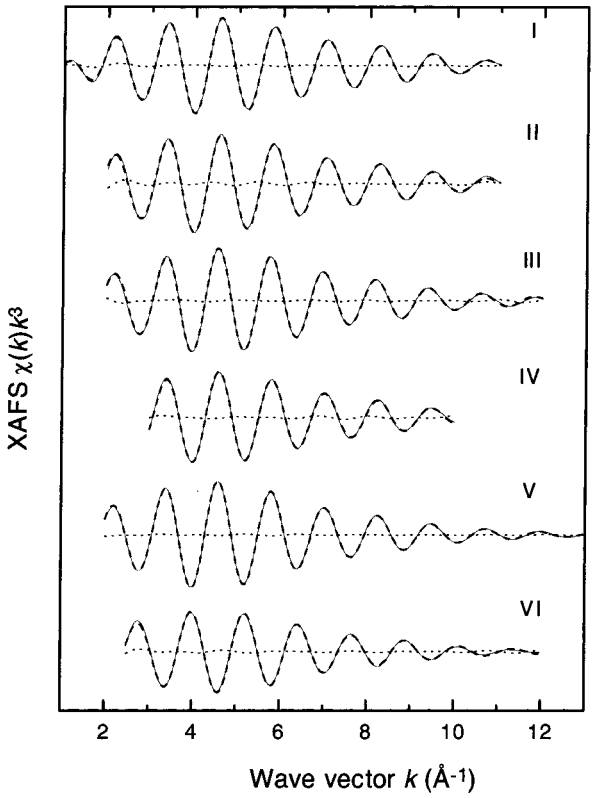

Figure 7. Comparison between the experimental XAFS spectra $\chi(k)$-k^3 after first shell filtering (—) and the corresponding spectra, calculated from the parameters presented in Table 3 (− − −). Residual curves are also represented (···).

the unfiltered data, we proceeded in the following manner: $f(\pi,k)$ and $\phi(\pi,k)$ functions were extracted from the filtered ESRF XAFS spectra considering the N, R, and DW (C_2) values presented in Table 3. A final refinement was then performed for each ion on the original unfiltered XAFS spectrum using these $f(\pi,k)$ and $\phi(\pi,k)$ functions (Figure 8). We consider the resulting parameters (Table 4) as the most reliable values for both aqua ions. As one can see, an excellent agreement is obtained between the filtered and unfiltered fitted data for both Sr^{2+} and Eu^{2+} ions.

The final results (unfiltered data) are summarized in Table 4 alongside those found in the literature for the Sr^{2+} aqua ion. Most of the authors[15,17,20,21] used the strontium oxide SrO as a reference compound, with a 6-coordinated strontium atom, and a Sr−O distance of 2.570 Å. Pfund et al.[15] used the ratio method and very narrow FT and fitting ranges, because of their high-pressure experimental setup. A coordination number of 7.3 and a distance of 2.62 Å were found at room temperature. In a

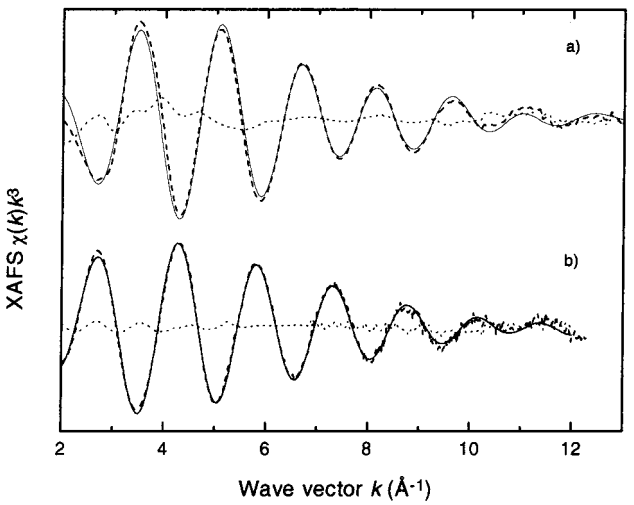

Figure 8. Final refinement (− −) performed on the original unfiltered XAFS spectrum $\chi(k)k^3$ (—) using filtered $f(\pi,k)$ and $\phi(\pi,k)$ functions for both Sr^{2+} (a) and Eu^{2+} (b) aqua ions. Residual curves are also represented (···).

second paper,[17] the same group used the harmonic Gaussian formalism with theoretical phase and amplitude based on a SrO-like cluster with the metal surrounded by 6 oxygen atoms at a distance of 2.60 Å, i.e., 0.03 Å higher than the crystallographic value. In this paper, a distance of 2.63 Å and a coordination number of 7.7 were found for the Sr^{2+} aqueous solution. Axe et al.[19] used a large FT range, and theoretical phase and amplitude based on a similar SrO-like cluster but with a Sr−O distance of 2.58 Å. They reported a fitted distance of 2.60 Å for the solid SrO and 2.62 Å for the Sr^{2+} solution. The C_3 and C_4 cumulant values found seem to be overestimated for the solution, and more especially for the cubic strontium oxide, a C_3 value of ca. 0.001 $Å^3$ corresponding to a distance shift of about 0.05 Å, due to the strong correlation between them. D'Angelo et al.[18] fitted the XAFS raw data (no FT) using a cluster based on a Molecular Dynamics simulation with a mean Sr−O distance of 2.63 Å and a mean coordination number of 9.8,[24] including the hydrogen atoms of the water molecules in their theoretical phase and amplitude calculations. The abnormally high coordination number of 10.3 is consistent with the long distance (2.643 Å) and with the important RDF asymmetry. Seward et al.[21] also fitted the XAFS raw data and used theoretical phase and amplitude based on a sequence of clusters derived from Molecular Dynamics simulations. A distance of 2.57 Å and a coordination number of 7.9 or 7.8 were obtained for the Sr^{2+} aqueous solution, depending if an asymmetric approximation was used or not. They concluded that the anharmonic effects were negligible. As a comparison, a distance of 2.56 Å and a coordination number of 5.9 were obtained for the SrO.

Instead of the SrO, Persson et al.[16] used the solid $[Sr(H_2O)_8](OH)_2$ as a reference compound. As already discussed, this compound is 8 coordinated, with a mean Sr−O distance of 2.619 Å. Having a first coordination sphere close to the one in solution, this compound is a better reference than the SrO for the Sr^{2+} aqua ion, and allows a better precision on fitted parameters. Persson et al.[16] used experimental phase and amplitude extracted from the solid $[Sr(H_2O)_8](OH)_2$, and found a distance value of 2.61 Å for the Sr^{2+} solution. However, they could not fit the coordination number because of the MET effects, and resolved to fix it to 8.

We used the reference compound suggested by Persson et al.,[16] and took into account the improvements presented in the literature today available, including the cumulant expansion, the MET subtraction, the phase-corrected Fourier filtration, the use of optimized theoretical phase and amplitude functions. Furthermore, we used large FT windows (0−14 $Å^{-1}$ in *k*-space), and slightly shorter fitting intervals to avoid the systematic errors introduced by the Fourier filtering procedure. These errors were estimated over the 2−13 $Å^{-1}$ fitting interval and a value of 1.5×10^{-4} was found, about 1 order of magnitude less than the fitting errors reported (Table 3). This, together with the excellent quality of the measurements performed in the ESRF, allowed us to gain an order of magnitude, both on fitting errors and statistical parameter incertitude (Table 4).

Figure 4a shows that the Sr^{2+} aqua ion environment in solution and in the solid octahydrated hydroxide are very similar, with coordination numbers in both states close to 8, and with a longer Sr−O distance in the solid by 0.016 Å (Table 3). The longer distance might be explained by the presence of the hydroxides counterions in the crystal 2nd shell. This difference is much smaller than the ionic radius difference (0.05 Å) for a one unit change in the coordination number.[13] The DW factor (C_2) of aqua ions in solution can be described as the sum of three terms: σ^2_{stat} due to static disorder, σ^2_{vib} due to thermal vibration and σ^2_{exch} due to the exchange of water molecules between the first and second hydration shells.[47] The larger DW factor (C_2) in solution indicates an increase of disorder in the liquid phase, and may also be related to the first coordination sphere water exchange rate. The radial distribution function (RDF) of the Sr^{2+} aqueous solution and of the $[Sr(H_2O)_8](OH)_2$ crystalline compound were simulated from the fitted parameters (Table 3), using both Gaussian and asymmetric approximation, and are compared in Figure 9. The C_3 cumulant measuring the skewing of distribution is rather low in both states, showing the small asymmetric character of the RDF. The C_4 cumulant which measures the weight in the tails of distribution was fitted and found negligible, corroborating D'Angelo's observation.[18] The asymmetry difference between the Sr^{2+} ion in the solid and solution states can be related to the disorder increase in solution.

In the solid $[Sr(H_2O)_8](OH)_2$, the $[Sr(H_2O)_8]^{2+}$ unit takes up a highly distorted square antiprismatic arrangement approaching a dodecahedral geometry.[6] This relatively unsymmetrical arrangement is related to the presence of the hydroxide anions in the 2nd coordination sphere of the solid. In solution, due to less constraints, the square antiprismatic arrangement is energetically favored,[48] and could therefore correspond to the optimum averaged representation of the $[Sr(H_2O)_8]^{2+}$ ion.

We found for the $[Sr(H_2O)_8](OH)_2$ crystalline reference, using theoretical phase and amplitude, a mean Sr−O distance of 2.615, very close to the 2.619 Å distance obtained by XRD at room temperature.[16] This confirms the reliability of our theoretical approach, together with the good concordance between results obtained using phases and amplitudes either calculated theoretically or extracted from a solid reference compound. It also justifies the theoretical approach used for our study of the Eu^{2+} ion in aqueous solution.

Results for the Eu^{2+} Aqua Ion. Shannon[13] published for the Eu^{2+} ion an ionic radius smaller by 0.01 Å than for the Sr^{2+} ion in the isomorphous solid chalcogenides. Recent XRD structural data for isostructural Eu^{2+} and Sr^{2+} oxygen bonded complexes give an Eu−O distance longer than the Sr−O distance by 0.011[49] and 0.015[50,51] Å. Hence the comparison of crystallographic data in the solid state shows that the metal−oxygen distance is the same for the Eu^{2+} and Sr^{2+}, within 0.02 Å for the same coordination number. Shannon[13] also suggested

TABLE 4: XAFS Structural Data for Sr^{2+} and Eu^{2+} Ions in Aqueous Solution: Final Results and Comparison with Literature[a]

sample	Δk	N	C_1 (Å)	R (Å)	C_2 (Å^2)	C_3 (Å^3) $\times 10^{-4}$	ref
			Sr^{2+} Solutions − Literature Data				
0.2 M $Sr(NO_3)_2$	2−5.8	7.3 (5)	2.62(3)				15
0.8 M $Sr(ClO_4)_2$[b]	2.5−14	8[d]		2.61(1)	0.0116(5)		16
0.2 M $Sr(NO_3)_2$[c]	2−5.8	7.7 (5)	2.63 (3)				17
0.1 and 3 M $SrCl_2$[c]	3−13/3−15	10.3 (1)	2.643 (2)		0.0210 (2)	β[e]	18
0.05 M $Sr(NO_3)_2$[c]	2.4−11.5	9 (1)	2.62 (2)		0.012(4)	9 (4)	19
0.1 M $SrCl_2$[c]	2.5−10.5	8.3 (7)	2.61 (2)		0.012		20
0.1 M $SrCl_2$[c]	2.5−9.5	7.8	2.57 (1)		0.010 (1)	B, C[e]	21
0.1 M $SrCl_2$[c]	2.5−9.5	7.9	2.57 (1)		0.012 (1)	B, C[e]	21
			Sr^{2+} and Eu^{2+} Solutions − Present Study				
0.14 M $Sr(O_3SCF_3)_2$	2−13	8.0 (3)	2.588 (3)	2.600 (3)	0.0126 (5)	2.7 (5)	-
0.15 M $Eu(O_3SCF_3)_2$	2−12	7.2 (3)	2.571 (3)	2.584 (5)	0.0138 (5)	1.5 (5)	-

[a] Δk is the fitting interval, N is the number of atoms located in the first shell at a distance R from the metal, C_1 is the first cumulant, $C_2 = \sigma^2$ is the DW factor, C_3 is the third cumulant characterizing the asymmetry of the RDF, and total errors are presented within brackets. [b] Analysis with experimental phase and amplitude. [c] Analysis with theoretical phase and amplitude. [d] Parameter fixed. [e] Parameters related to the RDF asymmetry.

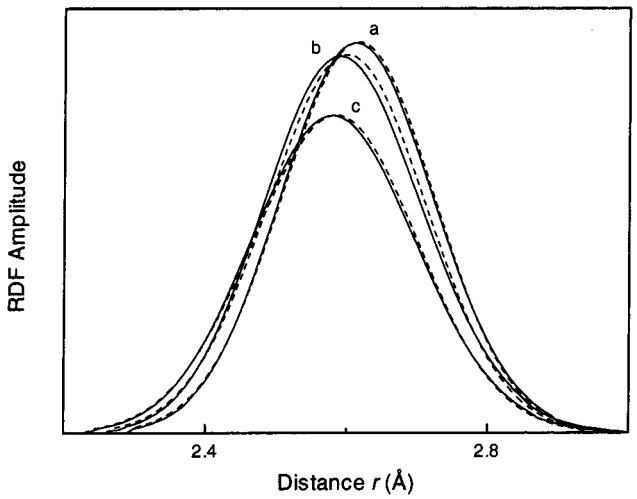

Figure 9. Reconstructed RDFs using both Gaussian (− − −) and asymmetric (—) approximations, of the first coordination shell of (a) solid $[Sr(H_2O)_8](OH)_2$, (b) Sr^{2+} in solution, and (c) Eu^{2+} in solution.

for both Eu^{2+} and Sr^{2+} ions an ionic radius difference of ca. 0.05 Å for a one unit change in the coordination number. In solution, the Eu−O distance is shorter than the Sr−O distance by 0.016 Å (Table 3). Within the experimental error, this difference is consistent with a conservation of the coordination number, or with a change of coordination number by less than one unit.

The phase-corrected FT of the Eu^{2+} and Sr^{2+} XAFS spectra in solution are compared in Figure 4b. As for Sr^{2+}, no contribution from the second hydration shell or multiple scattering is present in the FT of Eu^{2+}. The amplitude difference between Sr^{2+} and Eu^{2+} ions in aqueous solution (Figure 4b) comes from both a decrease in the coordination number from 8.0 to 7.2 and a 7% increase in the DW factor (C_2), as shown in Table 4. This increase of 0.0012 Å^2 in the DW factor can be interpreted as a large distribution of distance, due to the rather low degree of symmetry of a heptacoordinated polyhedron.[52] The equilibrium between the much more symmetrical coordination numbers 6 and 8 is not relevant since it would lead to an increase in the DW factor of 0.0100 Å^2, given the 0.05 Å ionic radius difference for a one unit change in the coordination number.[13] We therefore suggest an equilibrium between predominant 7 and minor 8 coordinated species, which would lead to a maximum DW factor increase of 0.0025 Å^2.

Considerations on partial molar hydration volumes V_i^0 led Persson et al.[16] to conclude that the hydration number in aqueous solution of the divalent alkaline earth metal ions decreases from

TABLE 5: Solid-State Coordination Numbers of Eu^{2+} and Eu^{3+} Ions in Acetates, Hydroxyacetates, and Oxalates from XRD Measurements[a]

aqua ion	acetate	hydroxyacetate	oxalate
Eu^{2+}	(8, 7)[53]; 8[50]; (8, 8)[54]	8[58]	(8, 8)[60]
Eu^{3+}	9[55]; (9, 9)[56]; (9, 9)[57]	9[59]	9[61]

[a] For crystalline structures where two different clusters are present in the unit cell, the coordination number within both clusters is given in parentheses.

8 for the large Ba^{2+} and Sr^{2+} ions, to ca. 7 for Ca^{2+}, 6 for Mg^{2+}, and finally 4 for Be^{2+}. Additionally, the XAFS measurements performed by Seward et al.[21] show, for the Sr^{2+} aqua ions in aqueous solution, a decrease in coordination number from 7.8 to 6.2 when increasing the temperature from 25 to 308 °C, with an intermediate 7-fold coordination at ca. 200 °C. This temperature increase is associated with a decrease of the Sr−O distance by 0.05 Å and an increase of the DW factor (C_2). Consequently, an heptacoordinated Eu^{2+} in aqueous solution would be structurally similar, in terms of first coordination sphere radius, to the Sr^{2+} ion, and similarly, in terms of coordination number, to the Ca^{2+} ion at room temperature and to the Sr^{2+} ion at higher temperature. However, even if Eu^{2+} and Sr^{2+} are not as similar in aqueous solution as they were thought to be, solid structures clearly show that they are very similar when coordinated with stronger and/or less flexible ligands.[49,50]

We now compare the Eu^{2+} ion (ionic radius of 1.25 Å)[13] and the Eu^{3+} ion (1.066 Å)[13] in aqueous solution. These two aqua ions present a difference in both ionic radii and charges that will influence the coordination number in two opposing ways. A larger ionic radius leads to more space around the ion and consequently to a higher coordination number. On the other hand, a lower charge will produce a weaker electric field and therefore a weaker attraction of the surrounding water molecules, i.e., a lower coordination number. It is a priori not obvious to decide which of these two effects will predominate. To solve that problem we have summarized in Table 5 the solid-state coordination numbers of Eu^{2+} and Eu^{3+} acetates,[50,53−57] hydroxyacetates,[58,59] and oxalates[60,61] obtained by XRD studies. The data show that there is a systematic one unit decrease in coordination number for the larger Eu^{2+} ion. This one unit difference in the solid state is also observed in aqueous solution. While Eu^{3+} occurs as an equilibrium between the $[Eu(H_2O)_8]^{3+}$ and the $[Eu(H_2O)_9]^{3+}$ ions, Eu^{2+} occurs in aqueous solution as an equilibrium between a predominant $[Eu(H_2O)_7]^{2+}$ and a minor $[Eu(H_2O)_8]^{2+}$ species.

A value of 4.4×10^9 s^{-1} has been measured by ^{17}O NMR[5] for the Eu^{2+} ion−water exchange rate in aqueous solution

assuming a coordination number of $N = 8$. Given the XAFS results, the change of coordination number from 8 to 7 would result in a water exchange rate k_{ex} of 5×10^9 s^{-1}, representing an increase of 14%. Furthermore, an increase of the rotational correlation time, τ_R, from 16.3 to 20.5 ps can be calculated from the change in coordination number and from the change in Eu−O distance from the assumed value of 2.63 to 2.584 Å as determined by XAFS. The large value of -11.3 cm^3 mol^{-1} for the volume of activation, $\Delta V^{\neq}$, for the water exchange reaction remains unchanged. This very negative volume leads to the attribution of a limiting associative mechanism. Supposing a coordination number of 7, this mechanism would suggest that the water exchange proceeds, for the $[Eu(H_2O)_7]^{2+}$ ion, through an 8-coordinate transition state (typically square antiprismatic[48]), possibly similar to the $[Sr(H_2O)_8]^{2+}$ ion structure in solution. The presence of an equilibrium between the coordination numbers 7 and 8 suggests that the energy difference between the $[Eu(H_2O)_7]^{2+}$ and $[Eu(H_2O)_8]^{2+}$ ions is small, as is the energy barrier for the water exchange reaction, resulting in a very fast water exchange rate.

Otherwise, Sham[47] pointed out that the ligand exchange rate constant, k_{ex}, in aqueous solution should be closely related to the DW factor (C_2) value. The large DW factor obtained in the present study for both the Eu^{2+} and Sr^{2+} ions are in good agreement with previously published results for other aqua ions, known to have very fast water exchange rates.[62,63]

Conclusion

Structural parameters of the Sr^{2+} ion in solution were reestablished by the XAFS method, taking into account all the improvements presented in the literature, including: the cumulant expansion, the MET subtraction, the phase-corrected Fourier filtration, the use of optimized theoretical phase, and amplitude functions. It allowed us to obtain a significant gain in the precision of the metal−oxygen distance and other structural parameters. The analysis with theoretical phase and amplitude was compared to an analysis where experimental phase and amplitude, extracted from the solid $[Sr(H_2O)_8](OH)_2$ reference compound, were used. The results showed good concordance. We obtained for the Sr^{2+} ion in aqueous solution a coordination number of 8.0, and an Sr−O distance of 2.600 Å.

This work establishes for the first time the Eu^{2+} ion structural parameters in aqueous solutions. The Eu^{2+} XAFS analysis was performed using a theoretical approach that was optimized for the Sr^{2+} aqua ion. We obtained an unexpected low coordination number of 7.2 together with an Eu−O distance of 2.584 Å. Whereas Eu^{3+} occurs as an equilibrium between the $[Eu(H_2O)_8]^{3+}$ and the $[Eu(H_2O)_9]^{3+}$ ions, Eu^{2+} occurs in aqueous solution as an equilibrium between a predominant $[Eu(H_2O)_7]^{2+}$ ion and a minor $[Eu(H_2O)_8]^{2+}$ species.

Acknowledgment. We thank Dr. Faysal Bouamrane, the ESRF BM29 beamline staff, and the LURE D42 beamline staff for their technical collaboration. We also thank the European Synchrotron Radiation Facility (ESRF) and the "Laboratoire pour l'Utilisation du Rayonnement Electromagnétique" (LURE) for the beamtime allocation and laboratory facilities. We finally acknowledge the Swiss National Science Foundation, the Latvian Science Foundation, the COST actions D9 (Advanced Computational Chemistry of Increasingly Complex Systems), and D18 (Lanthanide Chemistry for Diagnosis and Therapy) for financial support.

Supporting Information Available: Influence of the removal of the multielectron transition contributions, and of the photoelectron phase shift correction on the Fourier transform for an Sr^{2+} solution. This information is available free of charge via the Internet at http://pubs.acs.org.

References and Notes

(1) Powell, D. H.; Ni Dhubhghaill, O. M.; Pubanz, D.; Helm, L.; Lebedev, Y. S.; Schlaepfer, W.; Merbach, A. E. *J. Am. Chem. Soc.* **1996**, *118*, 9333.

(2) *The Chemistry of Contrast Agents in Medical Magnetic Resonance Imaging*; Merbach, A. E., Tóth, É., Eds.; John Wiley & Sons, Ltd.: Chichester, 2001.

(3) McCoy, H. N. *J. Am. Chem. Soc.* **1936**, *58*, 1577.

(4) Johnson, D. A. *Adv. Inorg. Chem. Radiochem.* **1977**, *20*, 1.

(5) Caravan, P.; Toth, E.; Rockenbauer, A.; Merbach, A. E. *J. Am. Chem. Soc.* **1999**, *121*, 10403.

(6) Richens, D. T. *The Chemistry of Aqua Ions*; Wiley & Sons: New York, 1997.

(7) Cossy, C.; Helm, L.; Powel, D. H.; Merbach, A. E. *New J. Chem.* **1995**, *19*, 27.

(8) Johansson, G.; Yokoyama, H. *Inorg. Chem.* **1990**, *29*, 2460.

(9) Stern, E. A.; Livins, P.; Zhang, *Z. Phys. Rev. B* **1991**, *53*, 798−805.

(10) Yamaguchi, T.; Nomura, M.; Wakita, H.; Ohtaki, H. *J. Chem. Phys.* **1988**, *89*, 5153.

(11) Solera, J. A.; Garcia, J.; Proietti, M. G. *Phys. Rev. B* **1995**, *51*, 2678.

(12) Antonio, M. R.; Soderholm, L.; Song, I. *J. Appl. Electrochem.* **1997**, *27*, 784.

(13) Shannon, R. D. *Acta Crystallogr.* **1976**, *A32*, 751.

(14) Seibig, S.; Toth, E.; Merbach, A. E. *J. Am. Chem. Soc.* **2000,** *122*, 5822.

(15) Pfund, D. M.; Darab, J. G.; Fulton, J. L.; Ma, Y. *J. Phys. Chem.* **1994**, *98*, 13102.

(16) Persson, I.; Sandstrom, M.; Yokoyama, H.; Chaudhry, M. *Z. Naturforsch.* **1994**, *50a*, 21.

(17) Palmer, B. J.; Pfund, D. M.; Fulton, J. L. *J. Phys. Chem.* **1996**, *100*, 13393.

(18) D'Angelo, P.; Nolting, H.-F.; Pavel, N. V. *Phys. Rev. A* **1996**, *53*, 798.

(19) Axe, L.; Bunker, G. B.; Anderson, P. R.; Tyson, T. A. *J. Colloid Interface Sci.* **1998**, *199*, 44.

(20) Parkman, R. H.; Charnock, J. M.; Livens, F. R.; Vaughan, D. J. *Geochim. Cosmochim. Acta* **1998**, *62*, 1481.

(21) Seward, T. M.; Henderson, C. M. B.; Charnock, J. M.; Driesner, T. *Geochim. Cosmochim. Acta* **1999**, *63*, 2409.

(22) Neilson, G. W.; Broadbent, R. D. *Chem. Phys. Lett.* **1990**, *167*, 429.

(23) Albright, J. N. *J. Chem. Phys.* **1972**, *56*, 3783.

(24) Spohr, E.; Palinkas, G.; Heinzinger, K.; Bopp, P.; Probst, M. M. *J. Phys. Chem.* **1988**, *92*, 6754.

(25) Bunker, G. *Nucl. Instrum. Methods* **1983**, *207*, 437.

(26) Sayers, D. E.; Bunker, B. A. In *X-ray Absorption*; Koningsberger, D. C., Prins, R., Eds.; Chemical Analysis Vol. 92; Wiley & Sons: New York, 1988. Crozier, E. D.; Rehr, J. J.; Ingalls, R. In *X-ray Absorption*; Koningsberger, D. C., Prins, R., Eds; Chemical Analysis Vol. 92; Wiley & Sons: New York, 1988.

(27) Rehr, J. J.; Mustre de Leon, J.; Zabinsky, S. I.; Albers, R. C. *J. Am. Chem. Soc.* **1991**, *113*, 5135.

(28) Dalba, G.; Fornasini, P.; Grisenti, R.; Purans, *J. Phys. Rev. Lett.* **1999**, *82*, 4240.

(29) Harrowfield, J. M.; Kepert, D. L.; Patrick, J. M.; White, A. H. *Aust. J. Chem.* **1983**, *36*, 483.

(30) Clerc, S. D.; Jewsbury, R. A.; Mortimer, M. G.; Zeng, J. *Anal. Chim. Acta* **1997**, *339*, 225.

(31) Villain, F.; Briois, V.; Castro, I.; Helary, C.; Verdaguer, M. *Anal. Chem.* **1993**, *65*, 2545.

(32) Kuzmin, A. *Physica B* **1995**, *208−209*, 175.

(33) Rocca, F.; Kuzmin, A.; Purans, J.; Mariotto, G. *Phys. Rev. B* **1994**, *50*, 6662.

(34) Benazeth, S.; Purans, J.; Chalbot, M.-C.; Nguyen-van-Duong, M. K.; Nicolas, L.; Keller, F.; Gaudemer, A. *Inorg. Chem.* **1998**, *37*, 3667.

(35) Dalba, G.; Fornasini, P. *J. Synchrotron Radiat.* **1997**, *4*, 243.

(36) Bunker, B. A.; Stern, E. A. *Phys. Rev. B* **1983**, *27*, 1017.

(37) Wortmann, G. *Hyperfine Interact.* **1989**, *47*, 179.

(38) Ravot, D.; Godard, C.; Achard, J. C.; Lagarde, P. In *Valence Fluctuations in Solids*; Falicov, L. M., Hanke, W., Maple, M. B., Eds.; North-Holland Publishing Company: Amsterdam, 1981; p 423.

(39) Tan, Z.; Budnick, J. I.; Luo, S.; Chen, W. Q.; Cheong, S. W.; Cooper, A. S.; Canfield, P. C.; Fisk, Z. *Phys. Rev. B* **1991**, *44*, 7008.

(40) Primak, W.; Kaufman, H.; Ward, R. *J. Am. Chem. Soc.* **1948**, *70*, 2043.
(41) Garske, D.; Peacor, D. R. *Am. Mineral.* **1961**, *46*, 189.
(42) Agron, P. A.; Busing, W. R. *Acta Crystallogr. C* **1986**, *42*, 141.
(43) De Villiers, J. P. R. *Am. Mineral.* **1971**, *56*, 758.
(44) Eick, H. A.; Baenziger, N. C.; Eyring, L. *J. Am. Chem. Soc.* **1956**, *78*, 5147.
(45) Mayer, I.; Levy, E.; Glasner, A. *Acta Crystallogr.* **1964**, *17*, 1071.
(46) Teo, B. K. *XAFS: Basic Principles and Data Analysis*; Springer-Verlag: Berlin, Heidelberg, New York, Tokyo, 1986.
(47) Sham, T. K. *Acc. Chem. Res.* **1986**, *19*, 99.
(48) Kepert, D. L. In *Aspects of the stereochemistry of 8-coordination*; Lippard, S. J., Ed.; Progress in Inorganic Chemistry, Vol. 24; Wiley & Sons: New York, 1978; p 179.
(49) Burai, L.; Toth, E.; Seibig, S.; Scopelliti, R.; Merbach, A. E. *Chem. Eur. J.* **2000**, *6*, 3761.
(50) Starynowicz, P. *Polyhedron* **1995**, *14*, 3573.
(51) Trunov, V. K.; Chubinidze, A. D.; Efremov, V. A.; Velikodni, Yu. A. *Koord. Khim.* **1984**, *10*, 403.
(52) Kepert, D. L. In *Aspects of the stereochemistry of 7-coordination*. Lippard, S. J., Ed.; Progress in Inorganic Chemistry, Vol. 25; Wiley & Sons: New York, 1979; p 41.
(53) Lossin, A.; Meyer, G. *Z. Anorg. Allg. Chem.* **1992**, *614*, 12.
(54) Starynowicz, P. *J. Alloys Compd.* **1998**, *268*, 47.
(55) Ganapathy, S.; Chacko, V. P.; Bryant, R. G.; Etter M. C. *J. Am. Chem. Soc.* **1986**, *108*, 3159.
(56) Yang, Y.; Luo, L.; Mak, T. C. W. *Chin. J. Struct. Chem.* **1988**, *7*, 1.
(57) Schleid, T.; Meyer, G. *Z. Naturforsch. B* **1989**, *44*, 1007.
(58) Starynowicz, P. *J. Alloys Compd.* **1998**, *275*−*277*, 815.
(59) Grenthe, I. *Acta Chem. Scand.* **1971**, *25*, 3347.
(60) Pink, H. *Z. Anorg. Allg. Chem.* **1967**, *353*, 247. Price, D. J.; Powell, A. K.; Wood, P. T. *Polyhedron* **1999**, *18*, 2499.
(61) Kahwa, I. A.; Fronczek, F. R.; Selbin J. *Inorg. Chim. Acta* **1984**, *82*, 161.
(62) Miyanaga, T.; Sakane, H.; Watanabe, I. *Bull. Chem. Soc. Jpn.* **1995**, *68*, 819.
(63) Helm, L.; Merbach A. E. *Coord. Chem. Rev.* **1999**, *187*, 151.